FULLERENES
AND ATOMIC CLUSTERS

An Electromechanical Nanothermometer
Based on Thermal Vibrations of Carbon Nanotube Walls

A. M. Popov[a], *, Yu. E. Lozovik[a], **, E. Bichoutskaia[b], G. S. Ivanchenko[c],
N. G. Lebedev[c], and E. K. Krivorotov[d]

[a] Institute of Spectroscopy, Russian Academy of Sciences, Troitsk, Moscow oblast, 142190 Russia
*e-mail: popov@ttk.ru
** e-mail: lozovik@isan.troitsk.ru
[b] Department of Chemistry, University of Nottingham, University Park, Nottingham, NG7 2RD United Kingdom
[c] Volgograd State University, Vtoraya Prodol'skaya ul. 30, Volgograd, 400062 Russia
[d] Moscow State Pedagogical University, ul. Malaya Pirogovskaya 1, Moscow, 119991 Russia
Received March 11, 2008; in final form, May 19, 2008

Abstract—A new concept is proposed for an electromechanical nanothermometer. The temperature measurements are performed by measuring the conductivity of the nanosystem, which depends substantially on the temperature due to the relative thermal vibrations of nanoobjects forming the nanosystem. The possibility of implementing the proposed concept is demonstrated using double-walled carbon nanotubes as an example. The dependence of the interwall interaction energy on the relative displacement of the nanotube walls is calculated within the density-functional theory. The conductivity of the nanotubes is calculated in the framework of the two-band Hubbard model. The calculations of the wall interaction energy and the conductivity are used to estimate the sizes of the nanothermometers based on different double-walled carbon nanotubes. It is shown that the nanothermometer under consideration can be used for measuring the temperature in localized regions with sizes of the order of several hundred nanometers.

1. INTRODUCTION

In recent decades, rapid progress in the nanotechnology has provided the possibility of designing nanoelectromechanical systems in which elements of electric circuits represent progressively smaller nanoobjects, including single molecules. The operation of these nanoelectromechanical systems is based on changes in the characteristics of the system with a change in relative positions of nanoobjects on a subnanometer scale with respect to other elements of the electric circuit [1]. Unique electronic properties of carbon nanotubes [2] and the possibility of controlling the relative motion of carbon nanotube walls with an atomic force microscope [3, 4] make them promising for the use in nanoelectromechanical systems as movable elements and elements of the electric circuit at once. A number of nanoelectromechanical systems based on the interaction and relative motion of carbon nanotube walls have been proposed and operating characteristics have been calculated for these nanoelectromechanical system, such as a variable nanoresistor [5, 6], a stress nanosensor [7], and a nonvolatile memory cell [8, 9]. Moreover, nanomotors based on the relative rotation of carbon nanotube walls have been fabricated to date [10, 11].

In this paper, we propose a new concept of an electromechanical nanothermometer. The operation of the proposed nanothermometer is based on the measurement of the conductivity of a system of nanoobjects in the case where this conductivity depends substantially on the relative position of nanoobjects on a subnanometer scale and, hence, varies with an increase in the temperature due to the thermal vibrations of these nanoobjects. The possibility of implementing this concept is considered using the electromechanical nanothermometer based on $(n, n)@(m, m)$ double-walled carbon nanotubes as an example. We make the estimates of a variation in the conductivity of double-walled carbon nanotubes as a result of the thermal vibrations of the walls. The calculations of the sizes of the nanothermometers intended for measuring the temperature under different conditions demonstrate that their sizes are as small as several tens of nanometers.

The temperature dependence of the conductivity of a system with allowance made for thermal vibrations of their constituent nanoobjects can be represented in the form

$$G(T) = \frac{\int_{-\infty}^{\infty} G(\mathbf{q}, T) \exp(-U(\mathbf{q})/kT) d\mathbf{q}}{\int_{-\infty}^{\infty} \exp(-U(\mathbf{q})/kT) d\mathbf{q}}, \qquad (1)$$

where $G(\mathbf{q}, T)$ is the conductivity of the system at a fixed relative position of the nanoobjects, which are described by the coordinates $\mathbf{q}$, and $U(\mathbf{q})$ is the potential energy of the system. The system can be used for designing a nanothermometer based on the relative thermal vibrations of the constituent nanoobjects in the case where the following conditions are satisfied.

(1) The conductivity $G(\mathbf{q}, T)$ depends weakly on the temperature at a fixed relative position of the constituent nanoobjects (condition A).

(2) The conductivity $G(\mathbf{q}, T)$ depends substantially on the coordinates $\mathbf{q}$ (condition B).

(3) The characteristic amplitude of the thermal vibrations of the nanoobjects should be large enough to make the main contribution to the temperature dependence of the conductivity $G(\mathbf{q}, T)$ (condition C).

(4) The characteristic amplitude of the thermal vibrations of the nanoobjects should be sufficiently small so that the relative displacements of the nanoobjects do not disturb the normal operation of the nanothermometer (condition D).

Moreover, it is desirable, if not necessary, that the minimum of the potential energy $U(\mathbf{q})$ of the system, in the vicinity of which nanoobjects execute relative vibrations, should correspond to the extremum in the dependence of the conductivity on the coordinates $\mathbf{q}$ (condition E). In this case, any small displacements of the nanoobjects from the equilibrium position lead to changes in the conductivity of the same sign (either to a decrease or to an increase in the conductivity) and, hence, the contributions to the change in the conductivity from the thermal vibrations corresponding to different displacements are not cancelled out. It should be noted that the minimum of the potential energy $U(\mathbf{q})$ and the extremum of the conductivity $G(\mathbf{q})$ can coincide, in particular, in the case where this equilibrium position corresponds to a higher symmetry of the system.

According to the calculations [12, 13], the conductivity of double-walled carbon nanotubes depends significantly on the relative positions of their walls. Below, we demonstrate that all the aforementioned conditions can be fulfilled for the proposed scheme of the nanothermometer based on the double-walled carbon nanotubes with nonchiral commensurate walls. We consider two cases of the relative positions of the carbon nanotube walls.

(1) A telescopic system in which the inner wall is inserted over its certain length into an outer wall. In this case, the length of overlap of the walls is smaller than the length of each wall.

(2) A system with a shuttle in which the short wall (shuttle) overlaps with the long wall (inner or outer) over the entire length. In this case, the length of overlap of the walls is equal to the length of the short wall.

According to the calculations for both telescopic and shuttle systems, the dependence of the conductivity $G(z)$ on the relative position z of the walls along the axis of the double-walled carbon nanotube is a periodic function with a large amplitude of conductivity oscillations [12, 13]. This indicates that the condition A is fulfilled. For the telescopic system, the conductivity also depends on the length of the overlap of the walls [13]. Measurements of the temperature dependence of the conductivity of single-walled nanotubes showed that their conductivity does not depend on the temperature at $T > 80$ K [14]. The weak temperature dependence of the conductivity is explained by the fact that, in nanotubes, electrons move over mesoscopic distances in a ballistic regime [15]. The calculations performed in our paper demonstrate that the conductivity of double-walled carbon nanotubes with a fixed relative position of the walls depends weakly on the temperature at $T > 80$ K. This means that the condition B is satisfied. The relative position of the walls changes as a result of their thermal vibrations. Consequently, the conductivity of double-walled carbon nanotubes can depend significantly on the temperature, predominantly, due to the relative vibrations of the walls. In our work, the dependence of the interwall interaction energy U for double-walled carbon nanotubes on the relative position z of the walls along the carbon nanotube axis is calculated using the density-functional theory. This dependence is used to evaluate the possibility of satisfying the conditions C and D, as well as to calculate the minimum sizes of nanothermometers based on the double-walled carbon nanotubes with nonchiral commensurate walls for which the relative diffusion of the nanotube walls does not disturb the operation of the nanothermometer. The analysis of the symmetry of double-walled carbon nanotubes with nonchiral commensurate walls shows that the additional condition E also holds true for these nanotubes. The general concept proposed in this work can stimulate the search for other nanosystems that can be used as an electromechanical nanothermometer.

In Section 2, the interwall interaction energy for double-walled carbon nanotubes is calculated using the density-functional theory. The conductivity of double-walled carbon nanotubes with a fixed position of the walls is calculated in Section 3. In Section 4, we describe the schematic diagrams of the nanothermometers based on double-walled carbon nanotubes, perform the evaluation demonstrating that the thermal vibrations make the main contribution to the conductivity of the nanothermometers, and calculate their operating characteristics. The advantages of the proposed design of the electromechanical nanothermometers over the nanothermometers based on the thermal expansion of liquids and advances in the development of nanotechnologies required for fabricating the electromechanical nanothermometers based on double-walled carbon nanotubes are discussed in Section 5.

2. CALCULATION OF THE INTERACTION BETWEEN NANOTUBE WALLS

The energy U of the interaction between two neighboring walls of a double-walled carbon nanotube depends on the coordinates describing the relative position of the walls: the angle ϕ of relative rotation of the walls about the nanotube axis and the relative displacement z of the walls with respect to this axis. The symmetry of the function $U(\phi, z)$ is uniquely determined by the symmetry of the double-walled carbon nanotube [16, 17]. Calculations of the interwall interaction energy and the analysis of the symmetry of double-walled carbon nanotubes demonstrate that two radically different cases are possible for the function $U(\phi, z)$. For double-walled carbon nanotubes with incommensurate walls [5, 6] or commensurate walls of which even one wall is chiral [17−20], the barriers between minima of the interwall interaction energy $U(\phi, z)$ are negligible (see also the review [21]). Therefore, the relative diffusion of walls in these double-walled carbon nanotubes is possible even at low temperatures and, hence, they cannot be used for fabricating an electromechanical nanothermometer based on the relative thermal vibrations of the walls. For double-walled carbon nanotubes with nonchiral commensurate walls ($(n, n)@(m, m)$, $(n, 0)@(m, 0)$), the barriers between the minima of the interwall interaction energy $U(\phi, z)$ are high. In this paper, we consider the operation of the electromechanical nanothermometer with the use of the $(n, n)@(m, m)$ double-walled carbon nanotubes as an example. For these double-walled carbon nanotubes, expression for the Fourier expansion of the interwall interaction energy is represented in the form [16]

$$U(\phi, z) = \sum_{M, K(\text{odd}) = 1}^{\infty} \alpha_K^M \cos\left(\frac{2\pi}{l_c} Kz\right) \cos\left(\frac{nm}{N} M\phi\right)$$
$$\times \sin^2\left(\frac{\pi nm}{2N^2}\right) \qquad (2)$$
$$+ \sum_{M, K(\text{even}) = 0}^{\delta_z/2} \beta_K^M \cos\left(\frac{2\pi}{l_c} Kz\right) \cos\left(\frac{nm}{N} M\phi\right),$$

where N is the greatest common divisor of the numbers n and m and l_c is the length of the unit cell of the double-walled carbon nanotube. The even terms always enter into expansion (2), and the odd terms occur only if both ratios n/N and m/N are odd.

The amplitudes of the harmonics in expansion (2) decrease exponentially with an increase in the numbers of harmonics M and K [17, 18, 22]. Therefore, the interwall interaction energy $U(\phi, z)$ for the double-walled carbon nanotubes with nonchiral commensu-

rate walls can be interpolated using only the first two terms in expansion (2); that is,

$$U(\phi, z) = U_0 - \frac{\Delta U_\phi}{2} \cos\left(\frac{2\pi}{\delta_\phi} \phi\right) - \frac{\Delta U_z}{2} \cos\left(\frac{2\pi}{\delta_z} z\right), \quad (3)$$

where U_0 is the average interwall interaction energy; ΔU_ϕ and ΔU_z are the energy barriers to the relative rotation of the walls and their sliding along the nanotube axis, respectively; and $\delta_\phi = \pi N/nm$ and $\delta_z = l_c/2$ are the periods of the function $U(\phi, z)$ for the relative rotation of the walls and their relative displacement along the nanotube axis, respectively. The semiempirical calculations for several tens of double-walled carbon nanotubes with nonchiral commensurate walls showed that the energy $U(\phi, z)$ with the use of relationship (3) can be interpolated accurate to within approximately 1% [19].

The barrier ΔU_ϕ to the relative rotation of the walls is the barrier between the equivalent minima of the energy $U(\phi, z)$, which are separated by the period δ_ϕ. For the majority of double-walled carbon nanotubes with nonchiral commensurate walls, the greatest common divisor of the numbers n and m is $N = 1$ [19]. For these double-walled carbon nanotubes, the period δ_ϕ is small and the barrier ΔU_ϕ to the relative rotation of the walls according to the calculations is low (lower than 0.005 meV/atom for the calculations within the density-functional theory [20] and lower than 10^{-11} meV/atom for the calculations with semiempirical potentials [19]). A considerable barrier ΔU_ϕ occurs only for the $(5, 5)@(10, 10)$ and $(9, 0)@(18, 0)$ double-walled carbon nanotubes [7, 17, 19], which are characterized by $N = 5$ and 9, respectively. For the double-walled carbon nanotubes with $N = 1$, the dependence of the interwall interaction energy $U(\phi, z)$ on the angle ϕ can be ignored and this energy can be approximately written in the form

$$U(z) = U_0 - \frac{\Delta U_z}{2} \cos\left(\frac{2\pi}{\delta_z}\right). \qquad (4)$$

Expression (4) will be used in Section 4 for evaluating the contribution of the relative thermal vibrations of the nanotube walls to the temperature dependence of the conductivity of the nanothermometer. In our work, the adequacy of expression (4) is verified using the calculations performed within the density-functional theory for the $(6, 6)@(11, 11)$ double-walled carbon nanotube.

The interwall interaction energy $U(\phi, z)$ was calculated within the density-functional theory in the local density approximation with the AIMPRO code [23]. In the quantum-mechanical description, the pseudo-wave functions of each carbon atom are represented by five atom-centered Gaussian functions determined by the sum of spherical harmonics. The maximum angular momentum taken into account in the expansion of the exponential functions of the Gaussian functions

was $l = 1$ (i.e., we accounted for up to and including the d orbitals) and only the exponential functions with the largest and smallest compressibility coefficients were expanded up to the angular momentum $l = 1$ (i.e., with allowance made only for the s and p orbitals). The Brillouin zone was described by 18 k points in the direction of the principal axis of the nanotube. In this work, we used the Bachelet–Hamann–Schlüter pseudopotentials [24] and the Perdew–Wang functional describing the exchange interaction of electrons and their correlation [25]. The unit cell of the (6, 6)@(11, 11) double-walled carbon nanotube contained 68 carbon atoms. The structure of each wall was optimized separately. The interwall interaction energy was calculated with a fixed wall structure. The accuracy in the calculations of the total energy of the double-walled carbon nanotube was determined by the choice of the technique for optimizing the system and, in our calculations, was as high as 1 μeV/atom.

It is well known that the conventional method of the density-functional theory is not suitable for the description of weak van der Waals and dispersion interactions; however, it is these interactions that determine the physical nature of the interaction of neighboring graphite layers and carbon nanotube walls. In the study of the properties of nanostructures with a graphite layer structure, the calculation method should account for both the strong interaction between carbon atoms inside the layer and the weak interaction between the layers. Satisfactory results can be achieved with the use of the density-functional theory, for example, by modifying the density functional. However, this approach is a serious and cumbersome quantum-mechanical problem. In our calculations, we do not modify the density functional but optimize the basis set (Gaussian functions) in such a way as to reproduce not only the energy properties but also the elastic properties of graphite with a high accuracy. The energy of the interaction between graphite layers (35 meV/atom) and the elastic coefficient $C_{44} = 4.20$ GPa corresponding to the relative shift of graphite layers, which were calculated with the optimized basis set [26], are in the excellent agreement with the experimental values of these quantities: 35 ± 10 meV/atom [27] and 5.05 ± 0.35 GPa [28], respectively. It should be noted that the calculations with the use of this method lead to interwall interaction energies of 23–25 meV/atom for a number of double-walled carbon nanotubes with an interwall distance of 3.4 Å, which corresponds to multiwalled carbon nanotubes. These energies are in the excellent agreement with the experimental data (23–33 meV/atom) for multiwalled nanotubes [4].

The interwall interaction energy for the (6, 6)@(11, 11) double-walled carbon nanotube was calculated for five different values of the relative displacement z of the walls with respect to the nanotube axis (including the relative position corresponding to the minimum energy of the interwall interaction) at a fixed angle ϕ of
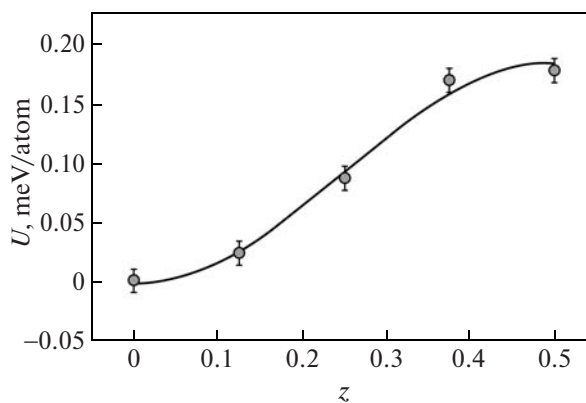
Fig. 1. The interwall interaction energy (in meV per atom of the outer wall) of the (6, 6)@(11, 11) double-walled carbon nanotube as a function of the displacement z of the walls along the nanotube axis. The displacement z is expressed in units of the period δ_z of the interwall interaction energy $U(z)$. Points indicate the calculated values of the energy. The solid line represents the interpolation of the energy by expression (4). The interaction energy and the relative displacement of the walls are reckoned from the minimum of the interaction energy (i.e., $U(0) = 0$).

the relative rotation of the walls about the axis. The calculated interwall interaction energy $U(z)$ (shown in Fig. 1) indicates that expression (4) is adequate within the accuracy of calculations.

It should be noted that relationships (2)–(4) hold true for any physical quantities dependent on the relative positions of nonchiral commensurate walls of double-walled carbon nanotubes, in particular, for the conductivity $G(\phi, z)$. This implies that both functions $U(\phi, z)$ and $G(\phi, z)$ have coinciding extrema and periods δ_ϕ and δ_z. Therefore, the additional condition E is satisfied for the double-walled carbon nanotubes with nonchiral commensurate walls.

3. CALCULATION OF THE CONDUCTIVITY OF DOUBLE-WALLED NANOTUBES

In this section, we consider the temperature dependences of the conductivity for the $(n, n)@(m, m)$ double-walled carbon nanotubes, which can be used for fabricating the nanothermometer, at fixed relative positions of the walls. Since single-walled nanotubes of this type exhibit a metallic conductivity [2], we can expect that the temperature dependence of the conductivity for the double-walled carbon nanotubes can also be characterized by a metallic conductivity. However, in this case, it is not ruled out that quantum effects can manifest themselves in particular temperature ranges, which, in turn, can result in phase transition of the metal–semiconductor type.

The electronic structure was simulated using the two-band Hubbard model modified with allowance made for electron hopping between walls of the double-walled carbon nanotube. The Hamiltonian of this

model for the double-walled carbon nanotube with the walls A and B can be written in the form [29]

$$
\hat{H} = -\sum_{j,\Delta,\sigma} t_{\Delta}^a (a_{j\sigma}^+ a_{j+\Delta,\sigma} + a_{j-\Delta,\sigma}^+ a_{j\sigma}) - \mu^a \sum_{j,\sigma} a_{j\sigma}^+ a_{j\sigma}
$$

$$
+ U \sum_j a_{j\sigma}^+ a_{j\sigma} a_{j,-\sigma}^+ a_{j,-\sigma}
$$

$$
- \sum_{j,\Delta,\sigma} t_{\Delta}^b (b_{j\sigma}^+ b_{j+\Delta,\sigma} + b_{j+\Delta,\sigma}^+ b_{j\sigma}) - \mu^b \sum_{j,\sigma} b_{j\sigma}^+ b_{j\sigma}
$$

$$
+ U \sum_j b_{j\sigma}^+ b_{j\sigma} b_{j,-\sigma}^+ b_{j,-\sigma} - \sum_{j,\zeta,\sigma} t_{\zeta}^{ab} (a_{j\sigma}^+ b_{j+\zeta,\sigma} + b_{j+\zeta,\sigma}^+ a_{j\sigma}),
$$

(5)

where t_{Δ}^a, t_{Δ}^b, and t_{ζ}^{ab} are the integrals of electron hopping between atoms of the wall A, atoms of the wall B, and the walls of the double-walled carbon nanotube, respectively; μ^a and μ^b are the chemical potentials of the walls A and B, respectively; U is the energy of the Coulomb interaction of electrons located at the same atom; $a_{j\sigma}^+$, $a_{j\sigma}$, $b_{j\sigma}^+$, and $b_{j\sigma}$ are the operators of production and annihilation of an electron with the coordinates $\mathbf{r}_j$ and the spin σ for the walls A and B, respectively; Δ is the distance between the neighboring carbon atoms in the corresponding nanotube walls; and ζ stands for the distance between the walls. The mutual arrangement of atoms in two walls of the double-walled carbon nanotube is described using the packing in which half the atoms of one wall are located directly above the atoms of the other wall and the second half the atoms are positioned above the centers of hexagons in the atomic structure of the neighboring wall.

In terms of Green's functions, the static electrical conductivity tensor has the form [30, 31]

$$
G_{\alpha\beta} = \frac{i\pi V}{kT} \langle \langle j_\alpha | j_\beta \rangle \rangle,
$$

(6)

where V is the nanotube volume and $\langle\langle j_\alpha | j_\beta \rangle\rangle$ is the Green's function for the current density vector $\hat{\mathbf{j}}$. The polarization vector $\hat{\mathbf{D}}$ and the current density vector $\hat{\mathbf{j}}$ are given by the formulas

$$
\hat{\mathbf{D}} = \frac{e}{V} \sum_{j\sigma} (\mathbf{r}_j a_{j\sigma}^+ a_{j\sigma} + \mathbf{r}_j b_{j\sigma}^+ b_{j\sigma}),
$$

(7)

$$
\hat{\mathbf{j}} = \frac{ie}{V} \sum_{k\sigma} [(\mathbf{v}^a a_{k\sigma}^+ a_{k\sigma} + \mathbf{v}^b b_{k\sigma}^+ b_{k\sigma})
$$

$$
+ \mathbf{v}^{ab} (b_{k\sigma}^+ a_{k\sigma} + a_{k\sigma}^+ b_{k\sigma})].
$$

(8)

Here, $\mathbf{v}^a$, $\mathbf{v}^b$, and $\mathbf{v}^{ab}$ are the electron velocities in the bands a, b, and ab, respectively. These velocities are represented in the following form:

$$
\mathbf{v}^a = \frac{1}{\hbar} \frac{\partial \varepsilon^a(\mathbf{k})}{\partial \mathbf{k}}, \quad \mathbf{v}^b = \frac{1}{\hbar} \frac{\partial \varepsilon^b(\mathbf{k})}{\partial \mathbf{k}},
$$

$$
\mathbf{v}^{ab} = \frac{1}{\hbar} \frac{\partial \varepsilon^{ab}(\mathbf{k})}{\partial \mathbf{k}}
$$

(9)

where ε^a, ε^b, and ε^{ab} are the dispersion relations for the electrons in the bands a, b, and ab, respectively, and $\mathbf{k}$ is the wave vector along the axis of the double-walled carbon nanotube.

Therefore, the problem regarding the determination of the conductivity tensor is reduced to the calculation of the two-particle Green's functions. The technique for calculating the isotropic conductivity as a function of the temperature was described in detail in [32]. In [32], it was revealed that the temperature dependence of the conductivity $G(T)$ for all the double-walled carbon nanotubes under consideration exhibits a specific behavior inherent in conductors. In other words, their conductivity decreases monotonically with an increase in the temperature. It should be noted that this result could be expected, because each wall in the double-walled carbon nanotubes has a metallic conductivity. In this case, the conductivity reaches saturation in the temperature range from 50 to 160 K, in which the dependence of the conductivity $G(T)$ becomes more flattened and then flattens out. The appearance of the plateau is explained by the more complex band structure of the double-walled carbon nanotubes as compared to the single-walled carbon nanotubes. However, the effects associated with the finite length of the walls of the double-walled carbon nanotubes were not considered in [32]. In our work, we use this technique for calculating the dependences of the conductivity $G(T)$ for a number of $(n, n)@(m, m)$ double-walled carbon nanotubes with a finite length of the outer wall, which can serve for the fabrication of the nanothermometer. The dependences $G(T)$ for the $(4, 4)@(10, 10)$ double-walled carbon nanotubes with an infinite inner wall and different lengths of the outer wall are plotted in Fig. 2. These dependences allow us to make the following inferences: (1) as for double-walled carbon nanotubes with an infinite outer wall, the dependence of the conductivity $G(T)$ exhibits a plateau in the temperature range $T = 50-160$ K, and (2) the conductivity of the double-walled carbon nanotubes changes insignificantly with a change in the length of the outer wall by several orders of magnitude. These inferences are valid for all the double-walled carbon nanotubes under consideration. The dependences of the conductivity $G(T)$ for different $(n, n)@(m, m)$ double-walled carbon nanotubes are compared in Fig. 3. It should be noted that dependences of the conductivity $G(T)$ for the $(5, 5)@(10, 10)$ and $(5, 5)@(11, 11)$ double-walled carbon nanotubes, as well as for the $(6, 6)@(11, 11)$ and $(6, 6)@(12, 12)$ double-walled carbon nanotubes, almost coincide with each other. Therefore, it can be
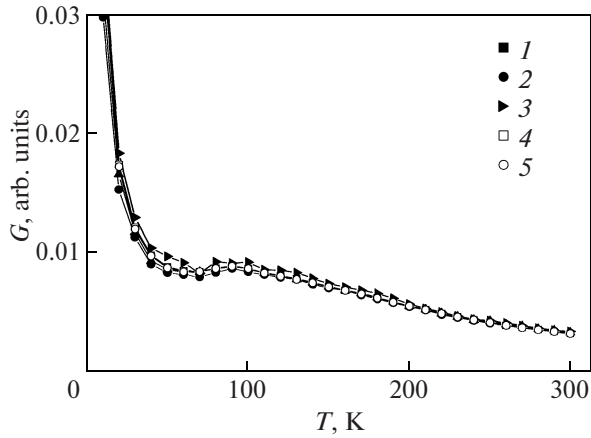
Fig. 2. Temperature dependences of the conductivity for the $(4, 4)@(10, 10)$ double-walled carbon nanotubes with different lengths L of the outer wall (in lengths l_c of the unit cells of the double-walled carbon nanotube). $L = (1)$ $10l_c$, (2) $30l_c$, (3) $50l_c$, (4) $100l_c$, and (5) $1000l_c$.
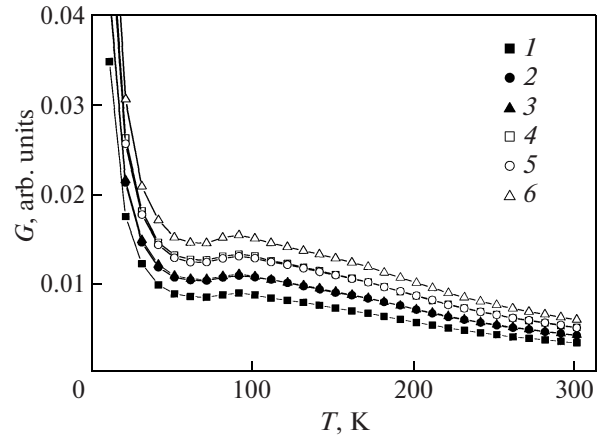
Fig. 3. Temperature dependences of the conductivity for different double-walled carbon nanotubes with an outer wall length of 100 unit cells: (1) $(4, 4)@(10, 10)$, (2) $(5, 5)@(10, 10)$, (3) $(5, 5)@(11, 11)$, (4) $(6, 6)@(11, 11)$, (5) $(6, 6)@(12, 12)$, and (6) $(7, 7)@(12, 12)$.

seen from Fig. 3 that the conductivity of the $(n, n)@(m, m)$ double-walled carbon nanotubes with a finite length of the outer wall is determined by the radius of the inner wall and depends weakly on the distance between the walls. These results agree with those for the infinite $(n, n)@(m, m)$ double-walled carbon nanotubes, for which the conductivity $G(T)$ increases with an increase in the radius of the double-walled carbon nanotube [32].

The performed calculations demonstrate that, for a fixed relative position of the walls, the conductivity $G(T)$ for the $(n, n)@(m, m)$ double-walled nanotubes with a finite length of the outer wall depends only slightly on the temperature at $T > 50$ K and that the dependence $G(T)$ exhibits a plateau in the temperature range $T = 50-160$ K. Therefore, we showed that the condition A required for using systems as a nanothermometer is satisfied for the system under consideration.

4. CALCULATIONS OF THE NANOTHERMOMETER CHARACTERISTICS

The schematic diagrams of the shuttle nanothermometer with a movable outer wall and the telescopic nanothermometer with a movable inner wall are depicted in Fig. 4. The systems of the shuttle nanothermometer with a movable inner wall and the telescopic nanothermometer with a movable outer wall are also possible.

Owing to the symmetry of double-walled carbon nanotubes with nonchiral commensurate walls, the extrema of the functions $U(z)$ and $G(z, T)$ coincide with each other. As was shown in Section 2, the interwall interaction energy $U(z)$ in the vicinity of the min-

imum can be interpolated by the relationship

$$U(z') = U_1 + \frac{\pi \Delta U_z}{\delta_z^2} z'^2, \qquad (10)$$

where U_1 is the minimum of the interwall interaction energy and z' is the displacement of the movable wall with respect to the position corresponding to this minimum. For small displacements z', the dependence of the relative position of the walls can be interpolated by the expression

$$G(z') = G_1(T)(1 + \gamma z'^2), \qquad (11)$$
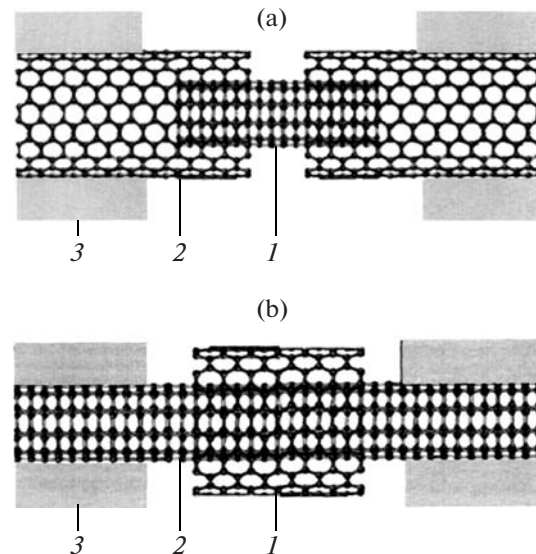
Fig. 4. Schematic diagrams of the nanothermometers based on double-walled carbon nanotubes: (a) the telescopic nanothermometer with a movable inner wall and (b) the nanothermometer with a movable shuttle in the form of an outer wall. Designations: (1) movable wall, (2) fixed wall, and (3) electrodes.

where G_1 is the conductivity of the double-walled carbon nanotube that corresponds to the minimum of the interwall interaction energy (i.e., the ground state of the system).

Substitution of relationships (10) and (11) into expression (1) gives the following formula for the temperature dependence of the conductivity of the nanothermometer:

$$G(T) = G_1(T)\left(1 + \frac{\gamma\delta_z^2 kT}{\pi\Delta U_z}\right) = G_1(T)(1 + H\Delta T). \quad (12)$$

The condition for a successful operation of the nanothermometer, according to which the thermal vibrations of the walls make the main contribution to the temperature dependence of the conductivity, is fulfilled when the following inequality holds true:

$$H\Delta T \gg \frac{\Delta G_1(T)}{\langle G_1(T)\rangle}, \quad (13)$$

where $\Delta G_1(T)$ is the difference between the maximum and minimum conductivities of the system in the ground state for the operating range ΔT of temperatures of the nanothermometer and $\langle G_1(T)\rangle$ is the average conductivity of the system in the ground state in the temperature range ΔT. By using the data presented in Figs. 2 and 3, we obtain the estimate

$$\frac{\Delta G_1(T)}{\langle G_1(T)\rangle} \sim 1 \quad (14)$$

for the operating temperature range of the nanothermometer $\Delta T = 250$ K from 50 to 300 K.

In order to evaluate the possibility of satisfying the condition G for the nanothermometer based on the (6, 6)@(11, 11) double-walled carbon nanotube, we use the data on the interwall interaction energy calculated in Section 2 and the conductivities calculated for this double-walled carbon nanotube in [12]. We interpolated the dependence of the conductivity of the (6, 6)@(11, 11) double-walled carbon nanotube on the relative position of the walls for the telescopic system in Fig. 3 from [12] with the use of relationship (11) and obtained the following estimates for the coefficient γ: $\gamma = 855 \pm 124$ Å^{-2} for a wall overlap length of 10 unit cells of the double-walled carbon nanotube and $\gamma = 21 \pm 12$ Å^{-2} for a wall overlap length of 250 unit cells. According to the first principles calculations (Section 2), the barriers to the relative motion of the walls along the nanotube axis are $\Delta U_z = 78.4$ meV and 1.96 eV for wall overlap lengths of 10 and 250 unit cells, respectively. For the operating temperature range $\Delta T = 250$ K, the products $H\Delta U$ are 117 ± 17 and 0.43 ± 0.10 for wall overlap lengths of 10 and 250 unit cells, respectively. Therefore, the obtained estimates indicate that the condition C is satisfied for small overlaps of the walls (several tens of unit cell lengths or several nanometers).

Let us estimate the minimum sizes of the electromechanical nanothermometer based on the double-walled carbon nanotubes with chiral commensurate walls for which the condition D can be satisfied. The condition D implies that the amplitude of the thermal vibrations of the short movable wall should be sufficiently small so that these vibrations do not disturb the normal operation of the nanothermometer. It is evident that the shorter the movable wall, the larger the amplitude of the thermal vibrations of this wall. An increase in the amplitude of the thermal vibrations can lead to the diffusion of the short movable wall along the fixed long wall. This diffusion is undesirable process, which can disturb the operation of the nanothermometer.

Now, we consider this diffusion for the system with the shuttle (Fig. 4b). The diffusion of the short movable wall (shuttle *1*) along fixed wall *2* does not disturb the nanothermometer operation only in the case where the displacement d of the shuttle due to the diffusion for the time t of the nanothermometer operation is smaller than the distance L_{es} between the shuttle and electrode *3*; that, is,

$$d = \sqrt{2Dt} < L_{es}, \quad (15)$$

where D is the diffusion coefficient for the shuttle motion along the fixed wall. The diffusion coefficient for the relative motion of the walls of the double-walled carbon nanotube is defined by the relationship [20]

$$D = A\exp\left(-\frac{BL}{T}\right), \quad A = \pi\delta_z\sqrt{\frac{\Delta U_z}{2m}},$$
$$B = \frac{\Delta U_z N_a}{l_m k}, \quad (16)$$

where m is the carbon atom mass, N_a is the number of atoms in the unit cell of the movable wall, l_m is the length of the unit cell of the movable wall, and L is the length of the movable wall. Substitution of expression (16) into relationship (15) gives the formulas for the minimum shuttle length

$$L = \frac{T}{B}\ln\left(\frac{2At}{L_{es}^2}\right) \quad (17)$$

and the total length of the nanothermometer between the electrodes

$$L_{nt} = \frac{T}{B}\ln\left(\frac{2At}{L_{es}^2}\right) + 2L_{es}. \quad (18)$$

The total length of the nanothermometer between the electrodes is minimum at $L_{es} = T/B$. This condition for the minimum length does not depend on the time of the nanothermometer operation.

Expressions (17) and (18) were used to calculate the total length of the nanothermometer and the

Characteristic sizes of the nanothermometers based on $(n, n)@(m, m)$ double-walled carbon nanotubes with a movable wall (shuttle) (L_{es} is the gap between the shuttle and the electrode, L is the shuttle length, L_{nt} is the total length of the nanothermometer between the electrodes, t is the time of the nanothermometer operation, and T is the operating temperature of the nanothermometer)

Nanotube	L_{es}, nm	$t = 10^{-6}$ s		$t = 100$ years	
		L, nm	L_{nt}, nm	L, nm	L_{nt}, nm
$T = 100$ K					
(4, 4)@(10, 10)	2.9 ± 1.1	15.5 ± 7.0	21.4 ± 7.0	120 ± 45	125 ± 45
(5, 5)@(11, 11)	2.0 ± 0.5	12.3 ± 3.5	16.3 ± 3.5	82 ± 21	85 ± 21
(6, 6)@(12, 12)	1.4 ± 0.3	10.1 ± 2.0	12.9 ± 2.0	60 ± 11	63 ± 11
(5, 5)@(10, 10)	0.36 ± 0.02	4.2 ± 0.2	4.9 ± 0.2	17.3 ± 0.8	18.0 ± 0.8
(6, 6)@(11, 11)	0.27 ± 0.01	3.2 ± 0.1	3.8 ± 0.1	12.8 ± 0.5	13.3 ± 0.5
(7, 7)@(12, 12)	0.19 ± 0.01	2.58 ± 0.07	2.96 ± 0.07	9.7 ± 0.3	10.0 ± 0.3
$T = 300$ K					
(4, 4)@(10, 10)	9.0 ± 3.5	27 ± 15	45 ± 15	340 ± 130	360 ± 130
(5, 5)@(11, 11)	5.9 ± 1.5	25 ± 8	36 ± 8	240 ± 60	245 ± 60
(6, 6)@(12, 12)	4.2 ± 0.8	21 ± 5	29 ± 5	170 ± 30	180 ± 30
(5, 5)@(10, 10)	1.1 ± 0.05	10.2 ± 0.5	12.4 ± 0.5	49.5 ± 2.5	51.5 ± 2.5
(6, 6)@(11, 11)	0.8 ± 0.02	7.9 ± 0.3	9.5 ± 0.3	36.6 ± 1.3	38.2 ± 1.3
(7, 7)@(12, 12)	0.6 ± 0.2	6.4 ± 0.2	7.6 ± 0.2	27.8 ± 0.7	29.0 ± 0.7

lengths of structural elements of this nanoelectromechanical system. For the (6, 6)@(11, 11) double-walled carbon nanotube, we used the barrier ΔU_z obtained in our work by extrapolating the dependence $U(z)$ with the use of relationship (4). For the other double-walled carbon nanotubes under consideration, we used the barriers ΔU_z calculated within the density-functional theory in our earlier work [33] as the difference between the energies for the relative positions of the walls that correspond to the extrema of the function $U(z)$. We analyzed the operation of the nanothermometer in two regimes, i.e., the pulsed measurement of the temperature for 10^{-6} s and the operation without failure for ten years. The results of the calculations are summarized in the table.

5. CONCLUSIONS

Thus, in the present paper, we considered the operation of the electromechanical nanothermometer based on the interaction between walls of double-walled carbon nanotubes. It was demonstrated that the nanothermometer can be used for measuring the temperature in spatially localized regions with sizes of several hundred nanometers. Since the measurement of the temperature by the nanothermometer under consideration is based on the measurement of the conductivity, the nanothermometer can be calibrated using a thermocouple. In this case, the accuracy in the measurement of the temperature with use of the nanothermometer, in principle, can be identical to that with the use of the thermocouple.

It should be noted that the electromechanical nanothermometer considered in this work differs fundamentally from the nanothermometer based on a nanotube filled with gallium [34, 35]. In the latter nanothermometer, the measurement of the temperature is based on the measurement of the length of a column of liquid gallium inside a carbon nanotube, which increases with an increase in the temperature due to the thermal expansion (in this case, the nanotube length is approximately equal to 10 μm). The measurement of the length of the gallium column requires the preliminary calibration and the subsequent identification of the nanothermometer with the use of transmission electron microscopy. As a consequence, the direct measurement of the temperature during the experiment becomes problematic. The electromechanical nanothermometer is free of the above disadvantage and, in particular, can be used as a component of nanoelectromechanical systems for measuring the temperature directly in their operation. Moreover, Schnidt et al. [36] considered the thermometer (approximately 1 μm in size) based on a superconductor–insulator–metal tunneling junction and intended for measuring temperatures <1 K. This differs substantially from the operating temperature range of the nanothermometer proposed in our work.

Let us discuss possible applications of the electromechanical nanothermometer based on nanotubes. These nanothermometers can be used in medical nanorobots [37] for determining the temperature of individual cells. A number of nanothermometers integrated into a microcircuit can be used for controlling the temperature distribution inside the microcircuit.

At present, considerable advances have been made in nanotechnologies, which provide a means for fabricating and operating nanoelectromechanical systems based on carbon nanotubes (see also the review [21]). In particular, a technique has been developed for measuring the conductivity of individual nanotubes. The motion of single-walled nanotubes and the relative motion of the walls in multiwalled nanotubes can be driven using nanomanipulators. It is also possible to remove caps from nanotube ends, to cut nanotube walls into parts of the required length, and to decrease the nanotube length. Nanotubes with a short outer wall (shuttle) have been prepared using the technique based on ohmic heating of nanotubes. Methods have been developed for uniquely determining the chiral indices of single-walled nanotubes and walls of double-walled nanotubes. Methods for preparing nanotubes with particular chiral indices are under development. All these facts taken together allow us to hope that the nanothermometer proposed in the present paper can be fabricated in the immediate future with the use of nanotechnologies.

ACKNOWLEDGMENTS

REFERENCES

1. H. Park, J. Park, A. K. L. Lim, E. H. Anderson, A. P. Aliviscatos, and P. L. McEuen, Nature (London) **404**, 57 (2000).

2. R. Saito, M. Fujita, G. Dresselhaus, and M. S. Dresselhaus, Appl. Phys. Lett. **60**, 2204 (1992).

3. J. Cumings and A. Zettl, Science (Washington) **289**, 602 (2000).

4. A. Kis, K. Jensen, S. Aloni, W. Mickelson, and A. Zettl, Phys. Rev. Lett. **97**, 025501 (2006).

5. Yu. E. Lozovik, A. V. Minogin, and A. M. Popov, Phys. Lett. A **313**, 112 (2003).

6. Yu. E. Lozovik, A. V. Minogin, and A. M. Popov, Pis'ma Zh. Éksp. Teor. Fiz. **77** (11), 759 (2003) [JETP Lett. **77** (11), 631 (2003)].

7. E. Bichoutskaia, M. I. Heggie, Yu. E. Lozovik, and A. M. Popov, Fullerenes, Nanotubes Carbon Nanostruct. **14**, 131 (2000).

8. L. Maslov, Nanotechnology **17**, 2475 (2006).

9. A. M. Popov, E. Bichoutskaia, Yu. E. Lozovik, and A. S. Kulish, Phys. Status Solidi A **204**, 1911 (2007).

10. A. M. Fennimore, T. D. Yuzvinsky, W. Q. Han, M. S. Fuhrer, J. Cumings, and A. Zettl, Nature (London) **424**, 408 (2003).

11. B. Bourlon, D. C. Glatti, L. Forro, and A. Bachtold, Nano Lett. **4**, 709 (2004).

12. I. M. Grace, S. W. Bailey, and C. J. Lambert, Phys. Rev. B: Condens. Matter **70**, 153405 (2004).

13. M. A. Tunney and N. R. Cooper, Phys. Rev. B: Condens. Matter **74**, 075406 (2006).

14. B. Gao, Y. F. Chen, M. S. Fuhrer, D. C. Glattli, and A. Bachtold, Phys. Rev. Lett. **95**, 196802 (2005).

15. *Carbon Nanotubes: Synthesis, Structure, Properties, and Applications*, Ed. by M. S. Dresselhaus, G. Dresselhaus, and P. Avouris (Springer, Berlin, 2001).

16. M. Damnjanović, I. Milošević, T. Vuković, and R. Sredanović, Phys. Rev. B: Condens. Matter **60**, 2728 (1999).

17. T. Vuković, M. Damnjavonić, and I. Milošević, Physica E (Amsterdam) **16**, 259 (2003).

18. M. Damnjanović, T. Vuković, and I. Milošević, Eur. Phys. J. B **25**, 131 (2002).

19. A. V. Balikov, Yu. E. Lozovik, A. G. Nikolaev, and A. M. Popov, Chem. Phys. Lett. **385**, 72 (2004).

20. E. Bichoutskaia, A. M. Popov, A. El-Barbary, M. I. Heggie, and Yu. E. Lozovik, Phys. Rev. B: Condens. Matter **71**, 113403 (2005).

21. Yu. E. Lozovik and A. M. Popov, Usp. Fiz. Nauk **177** (7), 786 (2007) [Phys.—Usp. **50**, (7), 749 (2007)].

22. M. Damnjanović, E. Dobardzić, I. Milošević, T. Vuković, and B. Nikolić, New J. Phys. **5**, 148.1 (2003).

23. P. R. Briddon and R. Jones, Phys. Status Solidi B **217**, 131 (2000).

24. G. B. Bachelet, D. R. Hamann, and M. Schlüter, Phys. Rev. B: Condens. Matter **26**, 4199 (1982).

25. J. P. Perdew and Y. Wang, Phys. Rev. B: Condens. Matter **45**, 13244 (1992).

26. R. H. Telling and M. I. Heggie, Philos. Mag. Lett. **83**, 411 (2003).

27. L. X. Benedict, N. G. Chopra, M. L. Cohen, A. Zettl, S. G. Lonie, and V. H. Crespi, Chem. Phys. Lett. **286**, 490 (1998).

28. C. S. G. Cousins and M. I. Heggie, Phys. Rev. B: Condens. Matter **67**, 024109 (2003).

29. Yu. A. Izyumov, M. I. Katsnel'son, and Yu. N. Skryabin, *Itinerant Electron Magnetism* (Fizmatlit, Moscow, 1994) [in Russian].

30. S. V. Tyablikov, *Methods in the Quantum Theory of Magnetism* (Nauka, Moscow, 1975; Plenum, New York, 1967).

31. A. A. Abrikosov, L. P. Gor'kov, and I. E. Dzyaloshinskii, *Methods of Quantum Field Theory in Statistical Physics* (Dover, New York, 1975; Dobrosvet, Moscow, 1998).

32. G. S. Ivanchenko and N. G. Lebedev, Fiz. Tverd. Tela (St. Petersburg) **49** (1), 183 (2007) [Phys. Solid State **49** (1), 189 (2007)].

33. E. Bichoutskaia, A. M. Popov, M. I. Heggie, and Yu. E. Lozovik, Phys. Rev. B: Condens. Matter **73**, 045435 (2006).

34. Y. Gao and Y. Bando, Nature (London) **415**, 599 (2002).

35. Y. Gao, Y. Bando, Z. Liu, D. Golberg, and H. Nakanishi, Appl. Phys. Lett. **83**, 2913 (2003).

36. D. R. Schnidt, C. R. Yung, and A. N. Cleland, Appl. Phys. Lett. **83**, 1002 (2003).

37. A. M. Popov, Yu. E. Lozovik, S. Fiorito, and L'Hocine Yahia, Int. J. Nanomed. **2**, 361 (2007).

Translated by O. Borovik-Romanova